ATLAS Internal Note
PHYS-NO-120
MUON-NO-222
17 February 1998

The inclusive muon cross-section in ATLAS

P. Eerola [1]
University of Helsinki, Helsinki, Finland

Abstract

The inclusive muon cross-section within the kinematical acceptance of the ATLAS detector was calculated using an up-to-date version of the PYTHIA simulation package. In the final results, muons from hadron decays and punch-through were also included.

[1] paula.eerola@helsinki.fi

1 Introduction

This note presents updated simulations of inclusive muon production from decays of heavy particles: b,c,t,W,Z^0. The simulations were performed using the PYTHIA simulation package. The previous results in the Muon Spectrometer section of the Technical Proposal [1, 2] were obtained with the ISAJET simulation program [3], while at present, the PYTHIA simulation package [4] has become a de facto standard in ATLAS, widely agreed to be the best understood and most versatile simulation program for describing generic hadron collisions. It should be noted that the physics simulations in the Technical Proposal, however, were performed using an older version of PYTHIA.

Compared to the simulations before the Technical Proposal, several input parameters have changed due to recent measurements from Tevatron, LEP and HERA, in particular: the masses of top, W, Z^0, and the widths of W and Z^0; masses, decay proper times and decay branching ratios of B-hadrons; new data to evaluate parton distribution functions.

Finally, the ATLAS muon spectrometer design and acceptance have evolved since the TP. In this study, the results are shown for the pseudorapidity acceptance of ± 2.7. The p_{T}-range of the muons was 3–50 GeV/c. The low-p_{T} cut-off corresponds roughly to the energy loss of the muons in the barrel calorimeters.

The counting rate in the muon spectrometer has major implications on the perfomance of the muon chambers, the trigger chambers and the muon trigger system, in particular the low-luminosity single muon trigger. The particle flux in the spectrometer consists of muons from decays of heavy particles (b,c,t,W,Z), muons from decays of hadrons (π,K), and punch-through particles from jets. The most important background comes from low-energy neutrons and photons, which originate from primary particle interactions with detector and accelerator elements close to the beam line.

The muon production from decays of primary J/ψ's was not considered in this study. The Tevatron J/ψ data has shown that the rate of muons from J/ψ decays is significantly higher than previously assumed. The theoretical modelling of primary J/ψ production is an active field of research. Estimates on the J/ψ production at LHC can be found for example in Ref. [5].

Each muon source is described in a separate chapter. For some cases, simulations were also performed at the Tevatron cms-energy to compare the results with CDF data.

The final results also include muon spectra from hadron decays and punch-through. These final results were the ones included in the ATLAS Muon Technical Design Report [6]. The hadron decays were simulated separately [7], and are not described here. After this note was completed, new results of hadron decays became available [8]. These new results were, however, not included here. The punch-through rates (shower muons, hadronic punch-through) were taken from the Technical Proposal [1].

2 Description of simulation

The PYTHIA version 5.7 was used for generating the event samples. The subversion used was 5.715, dated 24 Apr 1995. The default parton distribution function CTEQ2L was used, unless stated otherwise. For heavy quarks, the Peterson fragmentation fragmentation function was used.

The masses and decay times of B-hadrons were updated according to the latest Particle Data Group 1996 listings [9] with some exceptions. The B^{**} production was included using a tuning based on ALEPH data [10]. For the masses and widths of top, W and Z^0, more recent data from Tevatron and LEP were used [11, 12, 13].

The ATLAS event generation package ATGEN [14] was the framework used for event generation. Events satisfying particle level cuts (final state muon passing p_T and η-cuts $p_T > 3$ GeV/c, $|\eta| < 3$) were retained and output. In addition, for b and c, parton level cuts (p_T and η-cuts) were applied due to the divergence of the cross-section at vanishing p_T.

Most of the generated samples were stored on tape. The tape listing can be found in *http://wwwinfo.cern.ch/ eerola/tapes.html*, with links to the log-files, in which one can explicitly find the input parameters used, and the results of the event generation. An example for the datacards is listed in Appendix A.

3 b$\rightarrow \mu$X

Pairs of b-quarks were generated by switching on the following $2 \rightarrow 2$ processes in PYTHIA: $q_i q_j \rightarrow q_i q_j$ (ISUB=11), $q_i \bar{q}_i \rightarrow q_k \bar{q}_k$ (ISUB=12), $q_i \bar{q}_i \rightarrow gg$ (ISUB=13), $q_i g \rightarrow q_i g$ (ISUB=28), $gg \rightarrow q_k \bar{q}_k$ (ISUB=53), $gg \rightarrow gg$ (ISUB=68). No higher-order processes are included, but initial- and final-state radiation generate multijet events. The QCD matrix elements are given for massless quarks, and only final-state quarks are put on mass shell by hand. Therefore, the cross-sections are divergent at $p_T \rightarrow 0$, and a minimum p_T value for the hard scattering should be used. As a consequence, the total cross-section for b-quark pair production with $p_T \rightarrow 0$ is not a physically meaningful quantity.

There is an option in PYTHIA to generate massive quark pairs directly from a quark or a gluon fusion (ISUB=81,82). At LHC energies, however, it is expected that the majority of b-quark production originates from higher-order processes in the parton shower: gluon splitting $g \rightarrow b\bar{b}$, and flavour excitation $bg \rightarrow bg$. The only way in PYTHIA to account for these higher-order processes is to switch on general high-p_T jet production, and to select events containing a b-quark pair. This slows down the event generation, since only about one event in hundred contains a b-quark pair.

In order to check PYTHIA b-generation against data, and to understand possible differences resulting from different parton distribution functions, PYTHIA was run with Tevatron/CDF parameters: proton-antiproton collisions at $\sqrt{s} = 1.8$ TeV, $p_{\mathrm{T}}(\mathrm{b}) > 6.5$ GeV/c, $|\eta(\mathrm{b})| < 1$. The minimum p_{T} value for the hard scattering was set to 5 GeV/c, and the $|\eta|$-limit for the hard scattering was 5. No particle level cuts were applied since the simulation was performed at the parton level, without allowing for the partons to hadronize. The integrated cross-section of single b-quark production, shown in Fig. 1, shows good agreement between data and simulation. The data are from Ref. [15].

The parton distribution functions tested were: CTEQ2L, the present PYTHIA default (leading order), CTEQ2MS (next-to-leading order, singular at small x), and EHLQ1 and 2 (leading order, EHLQ1 was the old default). No model can be disqualified based on the CDF data shown in Fig. 1.

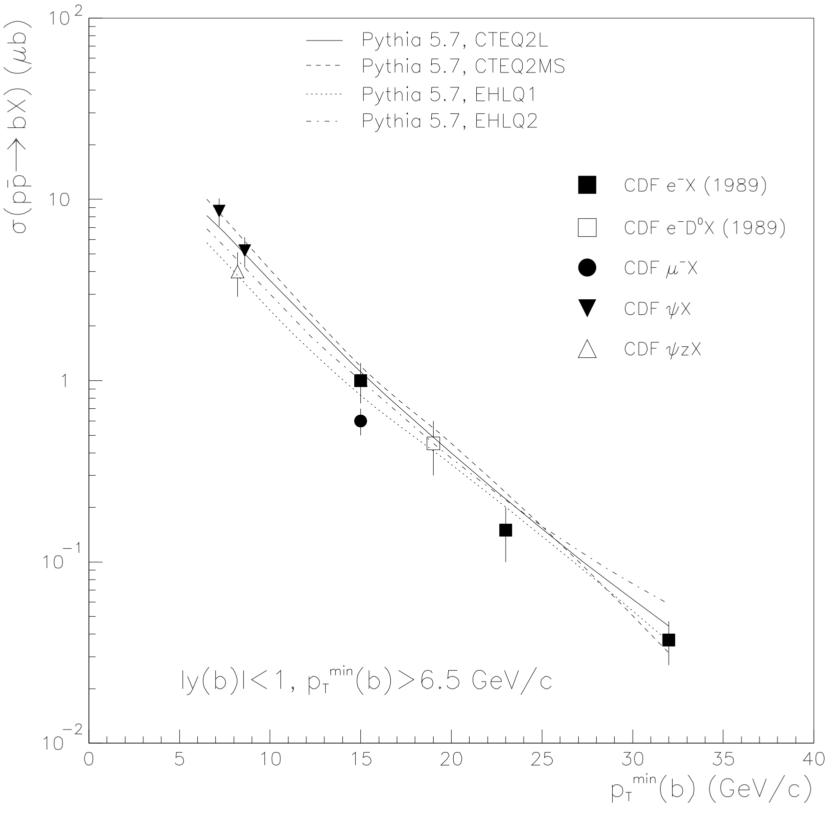

Figure 1: Comparison of PYTHIA5.7 with CDF data on single b-quark production.

Discrepancies between data and simulation results were found in correlated b-quark pair production. In Fig. 2 the total cross-section is shown for an event sample in which both the b- and the $\bar{b}$-quark were required to pass event selection cuts. The cuts were: $p_T(b), p_T(\bar{b}) > 6.5$ GeV/c, $|\eta(b)|, |\eta(\bar{b})| < 1$. The cross-section is shown as a function of the $p_T(\bar{b})$. The data are from Ref. [16]. Although the data statistics are poor, the simulation underestimates the overall rate roughly by a factor of two. The CDF collaboration found the same problem appearing with an exact next-to-leading order calculation; moreover, there are problems with the angular distributions of the two b-quarks. As shown in Fig. 2, the choice of the parton disribution function does not cure the problem.

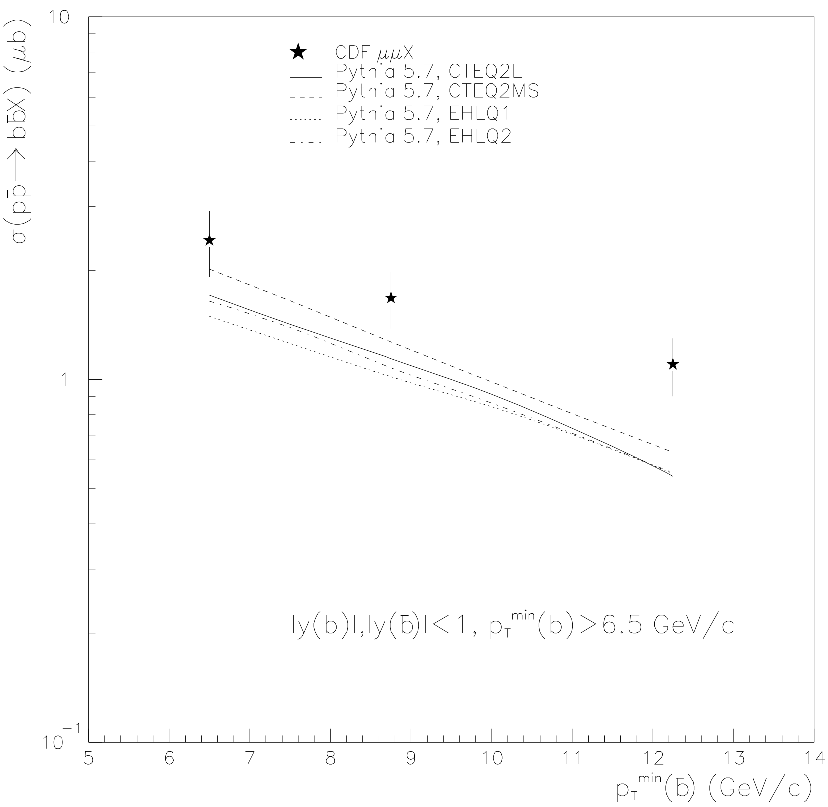

Figure 2: Comparison of PYTHIA5.7 with CDF data on correlated b-quark pair production.

The b-quark cross-sections were then compared at the LHC using the old and new PYTHIA default parton distribution functions, EHLQ1 and CTEQ2L. The following parameters and cuts were used: proton-proton collisions at $\sqrt{s} =$ 14 TeV, $p_T(b) > 10$ GeV/c, $|\eta(b)| < 2.5$. The minimum p_T value for the hard scattering was set to 10 GeV/c to speed up the generation, and the $|\eta|$-limit for the hard scattering was 5. Again, no particle level cuts were applied since the simulation was performed at the parton level. The results are shown in Fig. 3 for single b-quark production and in Fig. 4 for correlated b-quark pair production. The CTEQ2L can be seen to give softer spectrum for the single b-quark, and the maximum differences are about 25% between the cross-sections. The b-quark pair cross-sections agree well with each other.

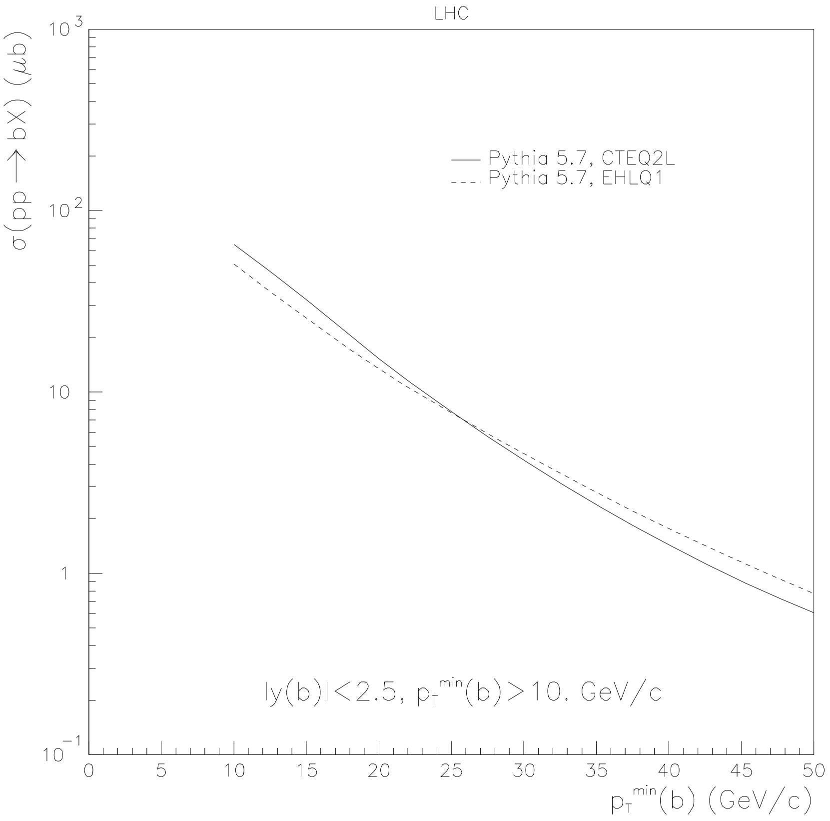

Figure 3: PYTHIA5.7 prediction of single b-quark production at LHC.

The generation of full events, including hadronization, proceeded as follows. Events had to first satisfy parton level cuts. The minimum p_{T} value for the hard scattering was set to 6 GeV/c, and the $|\eta|$-limit for the hard scattering was 5. It was then required that there was at least one b-quark in the event with $p_{\mathrm{T}} > 6$ GeV/c, $|\eta| < 5$. This event was then hadronized 10 times, and it was required that among the final state particles, there was a muon with $p_{\mathrm{T}} > 3$ GeV/c, $|\eta| < 3$. Peterson fragmentation was used, with $\varepsilon_{\mathrm{b}} = 0.006$. In the hadronization, no decays were forced, but the particles were allowed to be

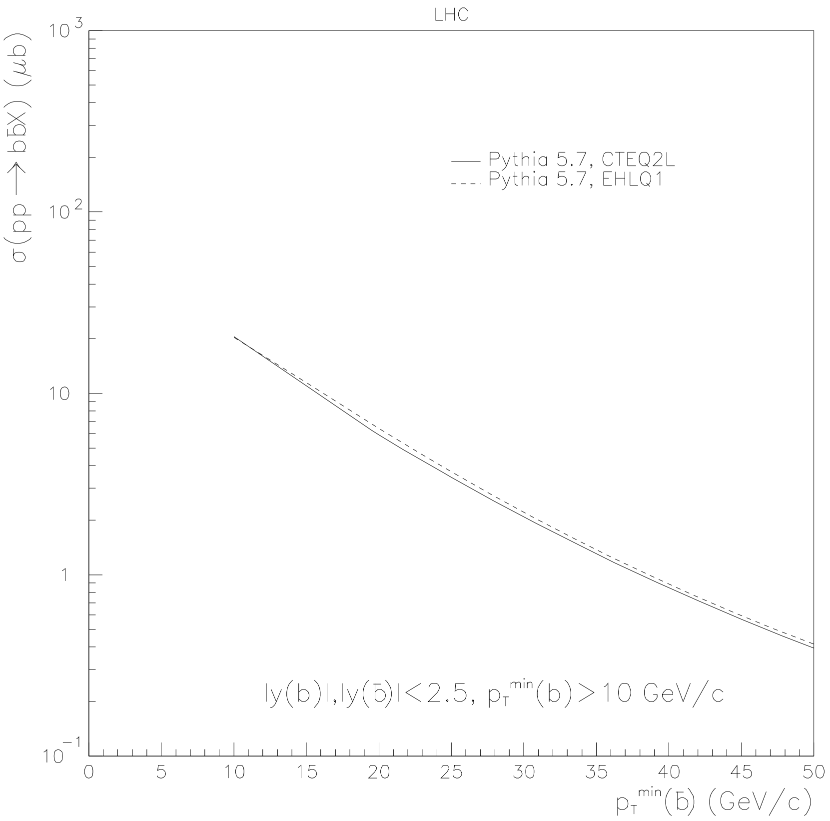

Figure 4: PYTHIA5.7 prediction of correlated b-quark pair production at LHC.

formed according to the standard branching fractions.

About 40,000 events were generated, with 30,000 of them written on tape (tapes LH3069-71, LH3078-80, with 5,000 events on each tape). The cross-section of the sample corresponded to 17.5 μb. The cross-section of a subsample with low-luminosity LVL1 trigger requirements, $p_{\mathrm{T}} > 6$ GeV/c, $|\eta| < 2.2$, was (2.25$\pm$0.10) μb, where the error is only the statistical error of the sample. The result is fully compatible with the cross-section used in the B-physics and Trigger sections of the Technical Proposal, which was 1.7 μb with $p_{\mathrm{T}} > 6$ GeV/c, $|\eta| < 1.6$, corresponding to 2.3 μb with a pseudorapidity acceptance of $|\eta| < 2.2$. The cross-sections were calculated separately hadronizing each event only once, not to introduce any biases from the looping procedure. The differential cross-sections are shown in Fig. 5.

The fraction of muons from direct b-decays $\mathrm{b} \to \mu\mathrm{X}$ was 85.6%. The fractions of muons from the following cascade decays were: $\mathrm{b} \to \mathrm{c} \to \mu\mathrm{X}$ 10.2%,

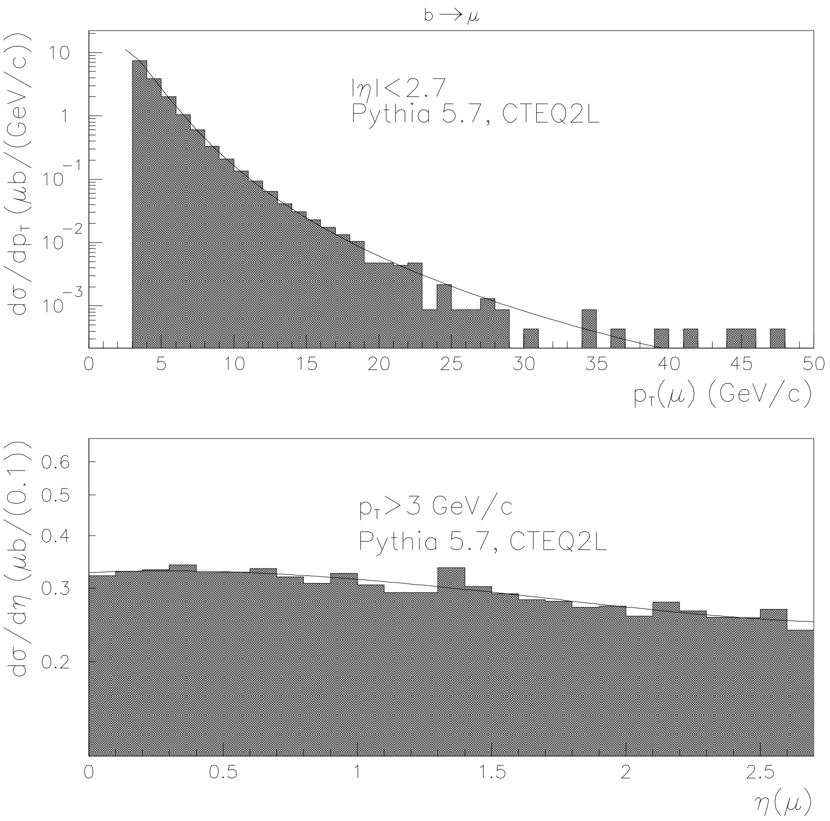

Figure 5: PYTHIA5.7 prediction for the muon p_{T}-spectrum (upper figure) and $|\eta|$-spectrum (lower figure) in $\mathrm{b\bar{b}}$-events.

$\mathrm{b} \to \mathrm{J}/\psi \to \mu\mathrm{X}$ 1.4%, $\mathrm{b} \to \tau \to \mu\mathrm{X}$ 1.6%. The fraction of muons from additional c-quarks in the same event was 1.1%.

4 c$\rightarrow$ μX

For c-quark pairs, the higher-order processes are even more important than for b-quark pairs. The generation of events was thus identical to the generation of b-events, except that a presence of a c-quark was required. Peterson fragmentation was used, with $\varepsilon_c = 0.07$. In the hadronization, no decays were forced.

About 25,000 events were generated, with 15,000 of them written on tape (tapes LH3072-74, with 5,000 events on each tape). The cross-section of the sample was 12.1 μb. The cross-section of a subsample with low-luminosity LVL1 trigger requirements, $p_T > 6$ GeV/c, $|\eta| < 2.2$, was (1.15$\pm$0.07) μb, where the error is only the statistical error of the sample. The cross-sections were calculated separately hadronizing each event only once. The differential cross-sections are shown in Fig. 6.

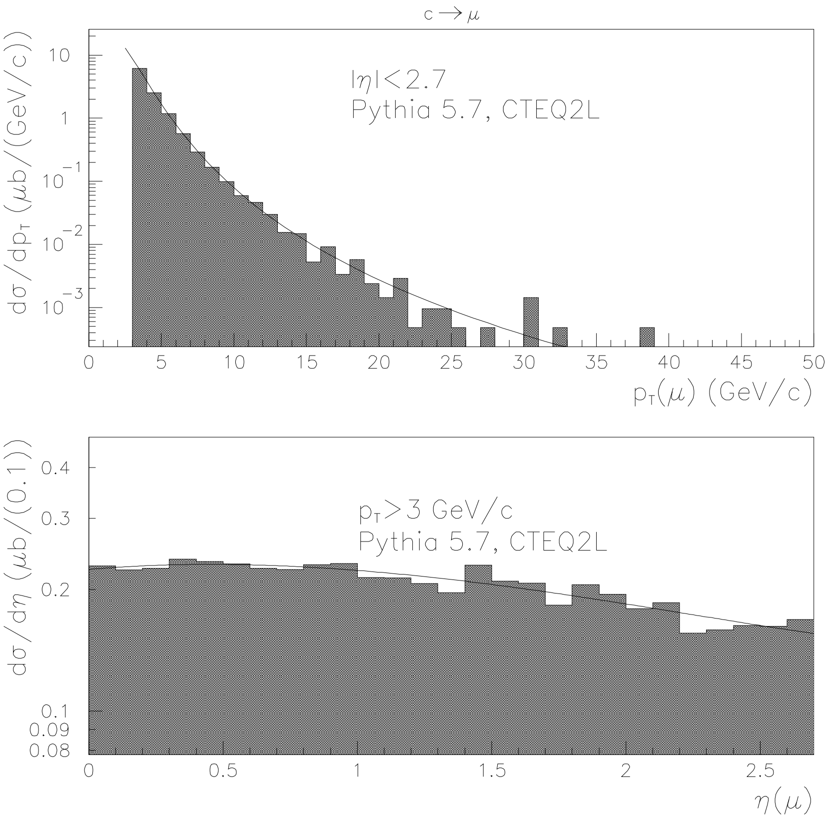

Figure 6: PYTHIA5.7 prediction for the muon p_T-spectrum (upper figure) and $|\eta|$-spectrum (lower figure) in c$\bar{c}$-events.

The fraction of muons from direct c-decays $c \to \mu X$ was 93.3%. The fractions of muons from additional b-quarks in the same event were: $b \to \mu X$ 5.4%, $b \to c \to \mu X$ 0.7%, $b \to J/\psi \to \mu X$ 0.1%, $b \to \tau \to \mu X$ 0.09%.

5 $\mathbf{t \to \mu X}$

Top-quark events were generated using the PYTHIA option to generate massive quark pairs directly from a quark or a gluon fusion (ISUB=81,82). Since massive matrix elements were used, no lower p_T cuts were necessary. The top mass was taken from recent CDF and D0 measurements to be 174 GeV/c^2 [11]. Peterson fragmentation was used, with $\varepsilon_t = 10^{-6}$. Since the event generation is fast using only the lowest-order production, each parton level event was hadronized only once, and no decays were forced in the hadronization phase.

About 24,000 events were generated and written on tape (tapes LH3060-65, with 4,000 events on each tape). The cross-section of the sample was 273.5 pb. The cross-section of a subsample corresponding to the low-luminosity LVL1 trigger requirements, $p_T > 6$ GeV/c, $|\eta| < 2.2$, was (156.5$\pm$1.2) pb, where the error is only the statistical error of the sample. The differential cross-sections are shown in Fig. 7.

The muons in top-quark events were found to originate from:
$t \to bW$, $W \to \mu X$ 42.5%, $t \to bW$, $W \to \tau \to \mu X$ 5.9%, $t \to bW$, $W \to c \to \mu X$ 7.0%, $t \to bW$, $b \to \mu X$ 44.6%. The last decay mode ($b \to \mu X$) includes both direct and cascade b-decays.

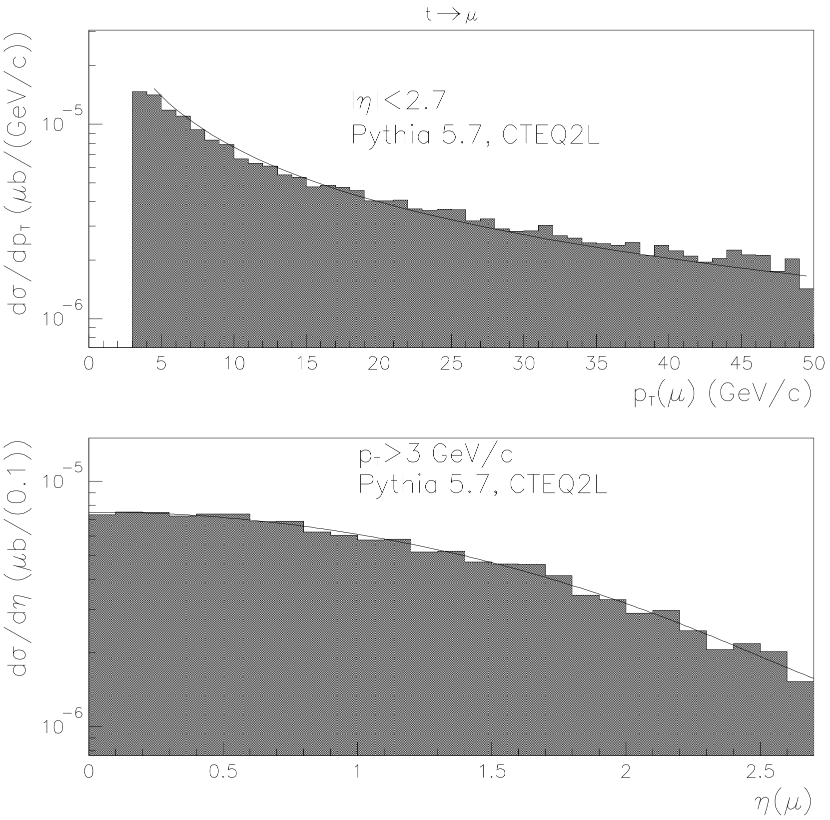

Figure 7: PYTHIA5.7 prediction for the muon p_{T}-spectrum (upper figure) and $|\eta|$-spectrum (lower figure) in $\mathrm{t\bar{t}}$-events.

6 W→ μX

Only the lowest order $2 \to 1$ resonance production of W was considered in the PYTHIA generation of the events, with initial state radiation switched on for generating additional jets via parton showering. In PYTHIA, the $2 \to 1$ resonance production with initial state radiation is considered to be the best option for inclusive Z/W generation at relatively low transverse momenta ($p_{\mathrm{T}} < m_{\mathrm{Z}}$). At higher transverse momenta, processes such as Z/W recoiling against a jet/photon ($2 \to 2$) become important. In PYTHIA, processes cannot be switched on simultaneously due to double counting.

Events were generated by switching on the following $2 \to 1$ processes in PYTHIA: MSEL=11 (ISUB=2, lowest order $2 \to 1$, $\mathrm{q_i \bar{q}_j} \to \mathrm{W}$). No K-factors were included. The W mass was taken from the LEP2 and Tevatron measurements, and the width was taken from Tevatron measurements [13].

In order to check PYTHIA simulation against data, PYTHIA was first run with Tevatron/CDF parameters: proton-antiproton collisions at $\sqrt{s} = 1.8$ TeV. No particle level cuts were applied since the simulation was performed at the parton level, without allowing for the W's to hadronize. The differential cross-section of W production, multiplied by the semileptonic branching fraction, is shown in Fig. 8. The integrated cross-section was $\sigma \cdot \mathrm{BR(e\nu)} = 1.79$ nb. The CDF measurement is $\sigma \cdot \mathrm{BR(e\nu)} = (2.49 \pm 0.12)$ nb. The data are from Ref. [17]. The CDF measurement is in good agreement with NNLO theoretical predictions and it seems, that PYTHIA underestimates the W rate by 30%, if one uses only the lowest order $2 \to 1$ production of W's.

Simulations of W production, with no hadronization, were also performed with a center-of-mass energy of 16 TeV in order to compare the present simulation results with the old calculations from the Aachen workshop [18], using full QCD corrections to order α_{s} and the DFLM set of structure functions. The simulation results are shown in Fig. 9. The total cross-section was 156 nb, to be compared with the old results in the Aachen proceedings of 172 nb, with a range of variation from 91 nb to 268 nb.

About 18,500 events were then generated with the LHC specifications and written on tape (5,500 events on the tape LH3075 and 6,500 events on tapes LH3076-7). The cross-section of the sample was 10.92 nb. The W was forced to decay into a pair of $\mu\nu_\mu$, and therefore, the cross-section includes the branching fraction of W→ $\mu\nu_\mu$, which was assumed to be Br(W→ $\mu\nu_\mu$) = 0.108. The cross-section of a subsample corresponding to the low-luminosity LVL1 trigger requirements, $p_{\mathrm{T}} > 6$ GeV/c, $|\eta| < 2.2$, was (7.77 ± 0.07) nb, where the error is only the statistical error of the sample. The differential cross-sections are shown in Fig. 10. The fraction of muons from W-decays was 100%.

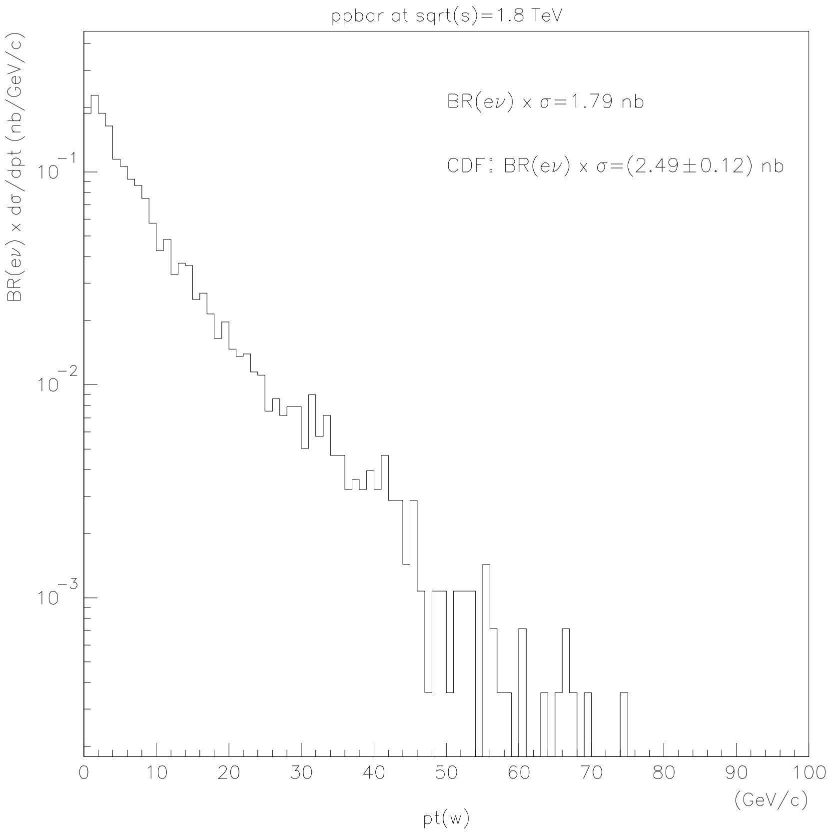

Figure 8: PYTHIA5.7 prediction of the differential W production cross-section at the Tevatron cms-energy. The total cross-section, multiplied by the semileptonic branching fraction, was 1.79 nb, to be compared with the CDF measurement of (2.49±0.12) nb.

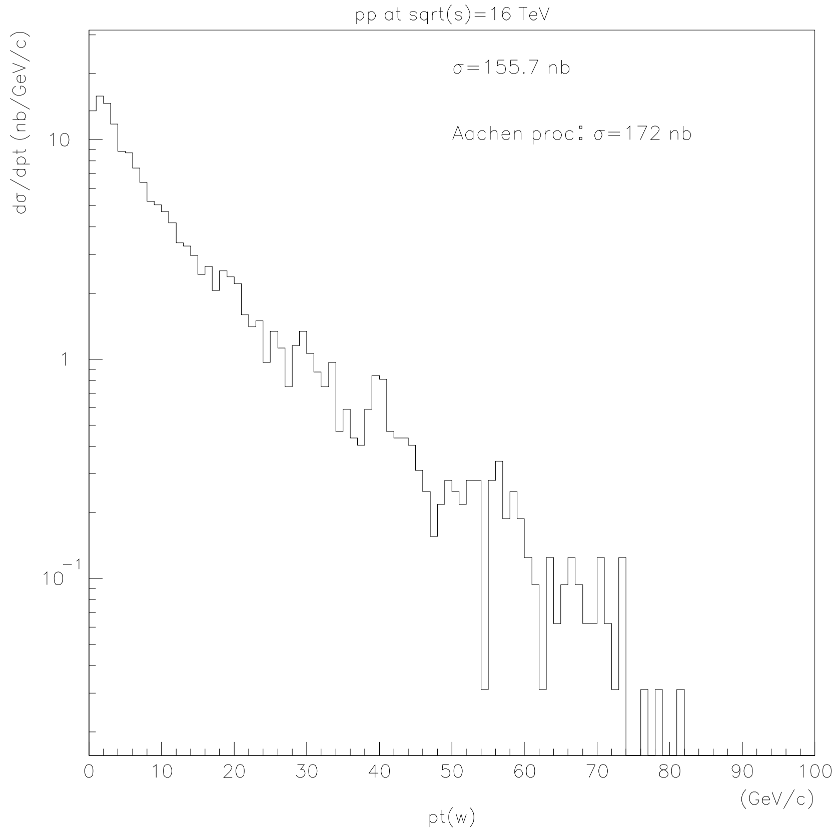

Figure 9: PYTHIA5.7 prediction of the differential W production cross-section at the cms-energy of 16 TeV.

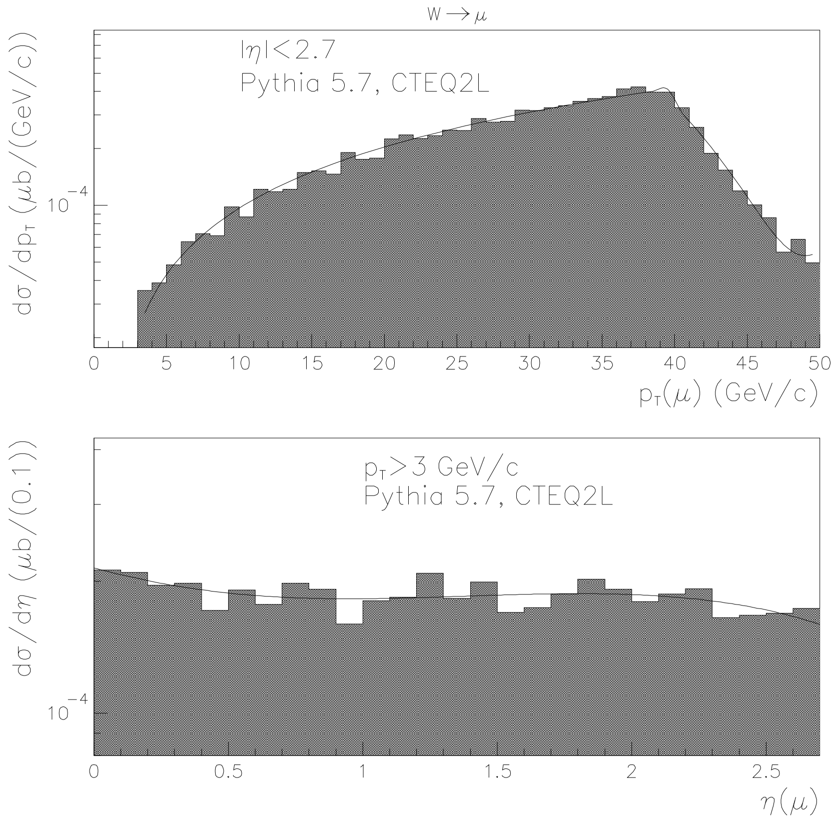

Figure 10: PYTHIA5.7 prediction for the muon p_{T}-spectrum (upper figure) and $|\eta|$-spectrum (lower figure) in W-events.

7 $Z/\gamma^* \to \mu X$

Similarly to the W$\to \mu$X decay, only the lowest order $2 \to 1$ resonance production of Z/γ^* was considered in the PYTHIA generation of the events, with initial state radiation switched on for generating additional jets via parton showering. Events were generated by switching on the following $2 \to 1$ processes in PYTHIA: MSEL=11 (ISUB=1, lowest order $2 \to 1$ $q_i\bar{q}_i \to Z^0/\gamma^*$), with a full Z/γ^* interference. No K-factors were included. The Z^0 mass and width were taken from the LEP data [12]. The Z^0 was forced to decay into a pair of muons.

About 19,500 events were generated and written on tape (tapes LH3066-68, with 6,500 events on each tape). The cross-section of the sample was 7.94 nb. Since the Z^0 was forced to decay into a pair of muons, the cross-section includes the branching fraction of $Z^0 \to \mu^+\mu^-$, which was assumed to be $\mathrm{Br}(Z^0 \to \mu^+\mu^-) = 0.03367$. The cross-section of a subsample corresponding to the low-luminosity LVL1 trigger requirements, $p_T > 6$ GeV/c, $|\eta| < 2.2$, was (1.84 ± 0.03) nb, where the error is only the statistical error of the sample. The differential cross-sections are shown in Fig. 11. The fraction of muons from Z^0-decays was 100%.

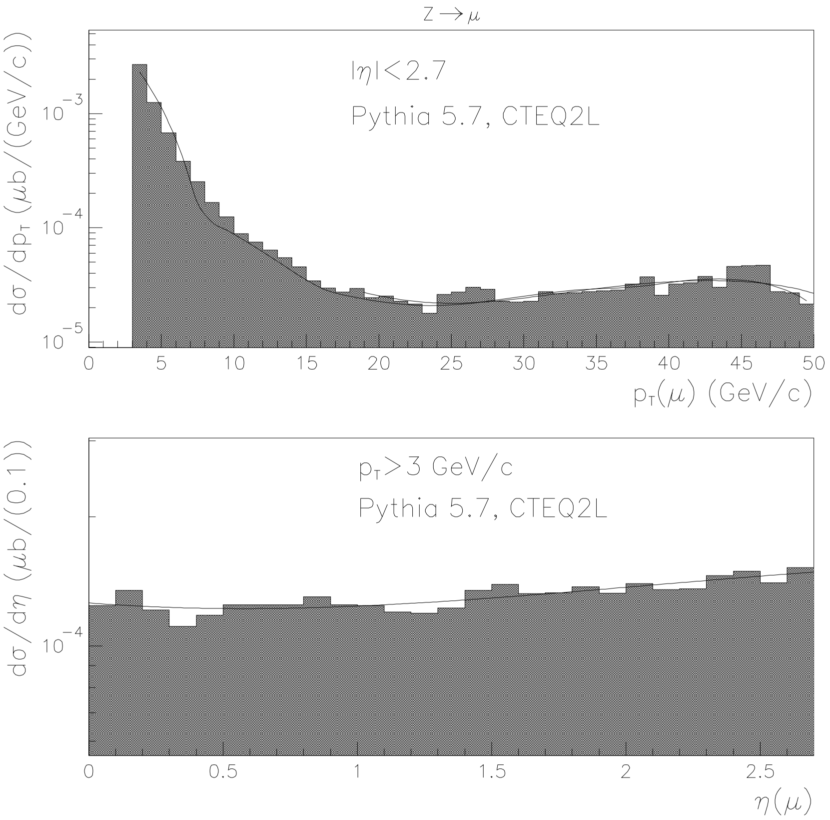

Figure 11: PYTHIA5.7 prediction for the muon p_{T}-spectrum (upper figure) and $|\eta|$-spectrum (lower figure) in Z^0-events.

8 Results

Figure 12 shows the transverse momentum spectrum of muons from heavy particle decays, hadron decays, shower muons and hadronic punch-through. At smallest values of transverse momenta ($p_{\mathrm{T}} < 8$ GeV/c) the muons from pion and kaon decays dominate. In the intermediate p_{T}-range (8 GeV/$c < p_{\mathrm{T}} < 30$ GeV/c) b- and c-quark decays dominate the muon rate, whereas at larger values of p_{T}, W and Z-decays give a sizeable contribution.

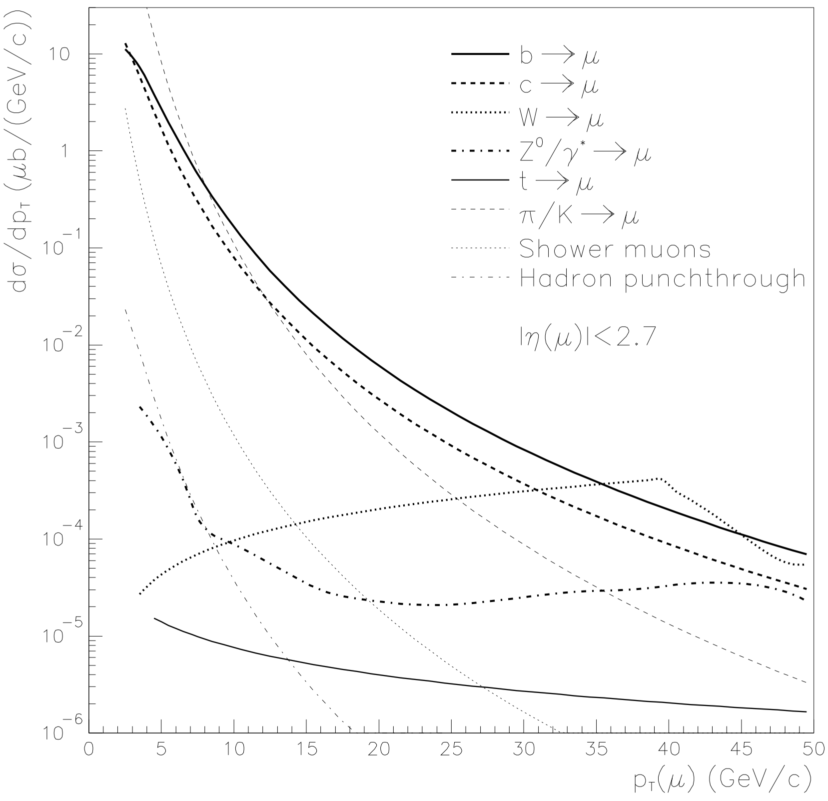

Figure 12: PYTHIA5.7 prediction of the differential cross-section $\mathrm{d}\sigma/\mathrm{d}p_{\mathrm{T}}$ of inclusive muon production LHC. The pseudorapidity range of the muons was $|\eta| < 2.7$. Contributions from hadron decays and punchthrough were obtained from Refs. [7] and [1], respectively.

In Figure 13, the pseudorapidity spectrum of muons from heavy particle decays and hadron decays is shown for muons with $p_{\mathrm{T}} > 3$ GeV/c. The hadron decay muons dominate the spectrum. It should be noted, however, that muons with 3 GeV/$c < p_{\mathrm{T}} <$ 5 GeV/c, will either be absorbed in the calorimeters or do not reach all the muon stations.

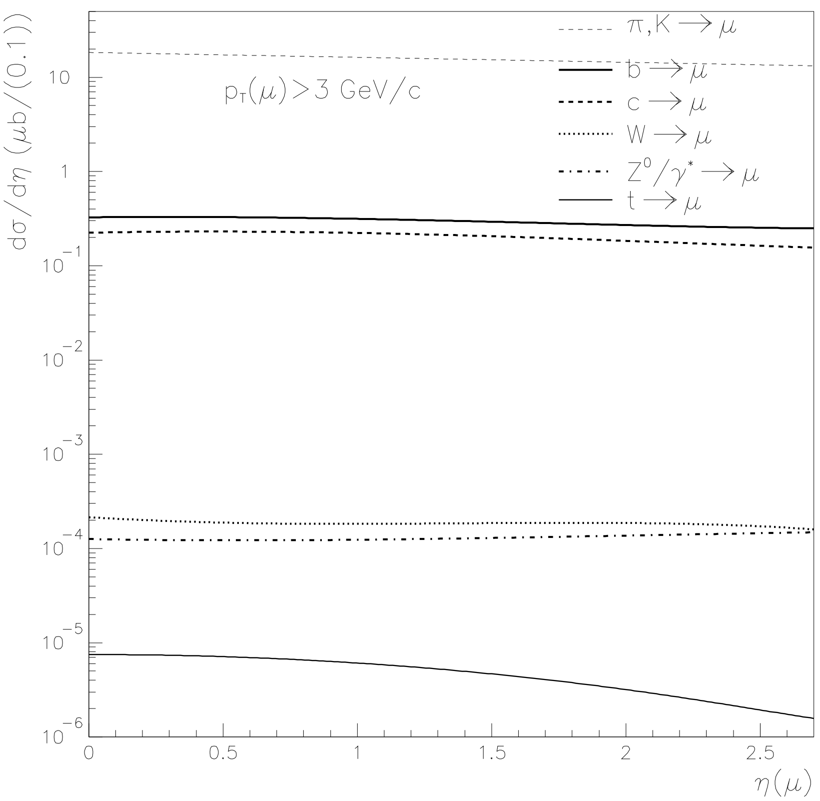

Figure 13: PYTHIA5.7 prediction of the differential cross-section dσ/dη of inclusive muon production LHC. The transverse momentum of the muons was greater than 3 GeV/c. Contribution from hadron decays was obtained from Ref. [7].

Figure 14 shows the integrated muon cross-section. The vector boson integrated cross-section should be considered with caution, since at high transverse momenta, processes such as Z/W recoiling against a jet/photon ($2 \to 2$), which were omitted in the simulation, become important and increase the cross-section at high transverse momenta.

The low-luminosity single muon trigger rates (L=10^{33} cm^{-2} s^{-1}) within the muon trigger acceptance ($p_{\mathrm{T}} >$ 6 GeV/c, $|\eta| < 2.2$) are shown in Table 1, together with the corresponding cross-sections. The total single muon trigger rate was found to be about 10 kHz, which is larger than the previous estimate of 8 kHz, due to the estimated increased hadron decay rate. The results in Table 1 were obtained by assuming sharp p_{T} thresholds, and the soft threshold behaviour of the trigger will increase the rates further.

Event class	The total cross-section [μb]	Trigger rate [Hz]
b$\rightarrow \mu$	2.25	2250
c$\rightarrow \mu$	1.15	1150
t$\rightarrow \mu$	0.0002	0.2
W$\rightarrow \mu$	0.008	8
Z$\rightarrow \mu$	0.002	2
π/K $\rightarrow \mu$	6.2	6200
Shower muons	0.04	40
Hadronic punchthrough	0.002	2
Sum	9.65	9650

Table 1: The total cross-section of inclusive muon production at LHC requiring $p_{\mathrm{T}} > 6$ GeV/c, $|\eta| < 2.2$, and the corresponding low-luminosity single muon trigger rates.

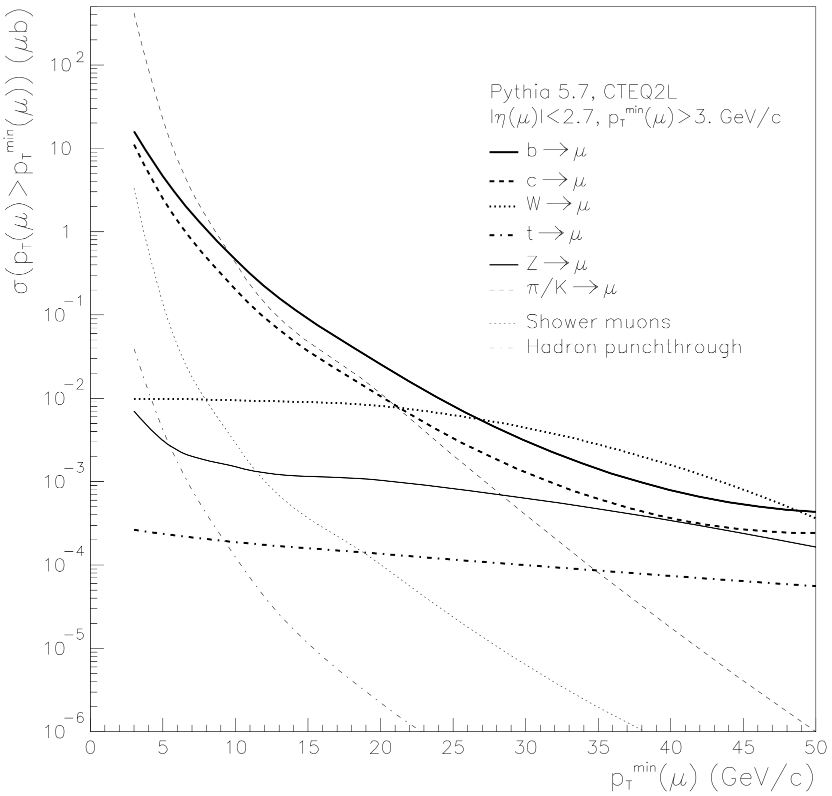

Figure 14: PYTHIA5.7 prediction of the integrated cross-section of inclusive muon production LHC. The transverse momentum of the muons was greater than 3 GeV/c, and the pseudorapidity range of the muons was $|\eta| < 2.7$. Contribution from hadron decays was obtained from Ref. [7] and contributions from shower muons and hadronic punch-through from Ref. [1].

9 Conclusions

This note presented updated PYTHIA simulations of inclusive muon production from decays of heavy particles: b,c,t,W,Z^0. Contributions from hadron decays in flight, shower muons and hadronic punch-through were included in the final results.

The muon cross-section from b-decays was found to be compatible with the previous ATLAS estimates. The recent CTEQ2L parton distribution function was seen to give a softer differential spectrum for the single b-quark than the previously used parton distribution function EHLQ, the maximum difference being about 25%. The total cross-sections agreed well with each other. PYTHIA could reproduce well the CDF data except for the correlated b-production.

The vector bosons were produced in the simulation using only the lower order process ($2 \to 1$), which is a valid approximation at low transverse momenta. At high transverse momenta, $2 \to 2$ processes become increasingly important, and therefore, the vector boson integrated cross-section should be considered with caution. The top-contribution has decreased compared to the previous estimates due to the high mass of the top quark.

The low-luminosity total single muon trigger rate was found to be 10 kHz instead of the 8 kHz previously estimated. The increase is mainly due to the increased rate of muons from hadron decays. These results do not yet include any threshold effects of the trigger.

References

[1] ATLAS Collaboration, 'ATLAS Technical Proposal', CERN/LHCC/94-43, LHCC/P2, December 1994.

[2] A. Cheplakov, A. Kriushin, V. Kukhtin and R. St.Denis, 'Muon Rates in ATLAS', ATLAS Internal Note Muon-NO-21 (1993).

[3] F.E. Paige and S.D. Proropopescu, in 'Physics of the Superconducting Super Collider 1986', eds. R. Donaldson and J. Marx (1987), p. 320.

[4] T. Sjöstrand, Computer Physics Commun. 82 (1994) 74.

[5] B. Cano-Coloma and M.A. Sanchis-Lozano, 'Charmonia Production in Hadron Colliders and the Extraction of Colour-Octet Matrix Elements', IFIC/97-29, FTUV/97-30, hep-ph/9706270, June 1997.

[6] ATLAS Collaboration, 'ATLAS Muon Spectrometer Technical Design Report', CERN/LHCC/ 97–22, ATLAS TDR 10, May 1997.

[7] The muon spectra from hadron decays were obtained from A. Ferrari and H. Ranft. The DPMJET II-simulation program was used for generating the events.

[8] A. Nisati and Y. Oren, private communication. Simulations were performed using the DPMJET and PYTHIA simulation programs. Some documentation can be found in *http://atlasinfo.cern.ch/Atlas/GROUPS/MUON/simulation/documents/pikdecay*.

[9] Review of Particle Physics, The Particle Data Group, Phys. Rev. D54 (1) 1996), *http://pdg.lbl.gov/*.

[10] P. Johnsson, 'A study of the use of the decay $\mathrm{B}^{**+} \to \mathrm{B}^{0(*)}\pi^+$ for $\mathrm{B}^0 - \bar{\mathrm{B}}^0$ tagging in ATLAS', ATLAS Internal Note PHYS-NO-073 (1995), *http://atlasinfo.cern.ch/Atlas/documentation/notes/PHYSICS/notes.html*.

[11] The top mass was chosen to be 174 GeV/c^2. In a recent review, G. Altarelli, 'The status of the Standard Model', CERN-TH/97-278, hep-ph/9710434, October 1997, the top mass was quoted to be (175.6 ± 5.5) GeV/c^2.

[12] The Z^0 mass and width were taken to be 91.186 GeV/c^2 and 2.4947 GeV/c^2, respectively. The most recent LEP electroweak working group report gives $m_\mathrm{Z} = (91.1867 \pm 0.0020)$ GeV/c^2 and $\Gamma_\mathrm{Z} = (2.4948 \pm 0.0025)$ GeV/c^2, assuming lepton universality (see The LEP collaborations, the LEP Electroweak Working Group and the SLD Heavy Flavour Group, 'A Combination of

Preliminary Electroweak Measurements and Constraints on the Standard Model', Internal Note LEPEWWG/97-02, August 1997, *http://www.cern.ch/LEPEWWG/stanmod/*).

[13] The W mass was taken to be 80.37 GeV/c^2. In the International Europhysics Conference on High Energy Physics, Jerusalem, August 1997, the W mass was quoted to be (80.43 ± 0.08) GeV/c^2 by D. Ward, 'Test of the Standard Model W mass and WWZ coupling', *http://www.cern.ch/hep97/abstract/tpl.htm*. The W width was taken to be 2.07 GeV/c^2 according to the 96 edition of the PDG [9].

[14] A. Amorim, ATLAS software group, 'ATGEN 2.0 User's Guide', ATLAS Internal Note SOFT-NO-033 (1996), *http://atlasinfo.cern.ch/Atlas/GROUPS/SOFTWARE/DOCUMENTS/ ATGENCGI/atgenman/atgenman/atgenman.html*.

[15] Compilation of the CDF b-quark integral cross-section measurements, see: *http://www-cdf.fnal.gov/physics/new/bottom/cdf1991/cdf1991.html*.

[16] F. Abe et al., CDF Collaboration, Phys. Rev. D55 (1997) 2546, *http://www-cdf.fnal.gov/physics/pub97/pub97.html*.

[17] F. Abe et al., CDF Collaboration, Phys. Rev. Lett. 76 (1996) 3070, *http://www-cdf.fnal.gov/physics/pub96/pub96.html*.

[18] T. Matsuura and H. Plothow-Besch, 'Total W and Z cross sections', in p. 94, Large Hadron Collider Workshop Proceedings, Vol. II, eds. G. Jarlskog and D. Rein, CERN 90-10, ECFA 90-133, December 1990.

A Example of input datacards

This is an example for the set of datacards used for generating decays W→ $\mu\nu^{-}$.

```
LIST
C Store events
TASK 1
TRIG -6500
DEBU 0 1 1
BACK 0
RNDM 4427331
ENER 14000.
FRAME 'CMS'
BEAM 'P' 'P'
C...try to circumvent LUDECY problem
MSTU 22=1000
C...C CHOOSE lowest order W PRODUCTION (ISUB=2), IS radiation on
MSEL 1=12
C Kinematic cuts
C CKIN   3=6.
C CKIN 9= -5.0 10= 5.0    11=-5.00  12=5.00
C Use Peterson fragmentation for heavy quarks
MSTJ 11=3
PARJ 54=-0.07   55=-.006  56=-.000001
C Turn off B mixing
MSTJ 26=0
C Top mass average from CDF+D0 summer 1996
PMA1 6=174.
C W mass LEP2+Tevatron average winter 1997, width PDG96
PMA1 24=80.37
PMA2 24=2.07
C Z mass and width LEP average winter 1997
PMA1 23=91.186
PMA2 23=2.4947
C-------------------------------------------------------------
C Force decay W->mu nu
*DMOD 24  172 0 0 0.0000
*DMOD 24  173 0 0 0.0000
*DMOD 24  174 0 0 0.0000
*DMOD 24  175 0 0 0.0000
*DMOD 24  176 0 0 0.0000
*DMOD 24  177 0 0 0.0000
*DMOD 24  178 0 0 0.0000
*DMOD 24  179 0 0 0.0000
*DMOD 24  180 0 0 0.0000
*DMOD 24  181 0 0 0.0000
*DMOD 24  182 0 0 0.0000
*DMOD 24  183 0 0 0.0000
*DMOD 24  184 0 0 0.0000
*DMOD 24  185 0 0 0.0000
*DMOD 24  186 0 0 0.0000
*DMOD 24  187 0 0 0.0000
*DMOD 24  188 0 0 0.0000
*DMOD 24  189 1 0 1.0000
*DMOD 24  190 0 0 0.0000
*DMOD 24  191 0 0 0.0000
C-------------------------------------------------------------
C Higgs mass
PMA1 25=300.
C-------------------------------------------------------------
C Masses and widths of B mesons (id. by compressed codes KC)
C Generic b-hadron lifetime, PDG96
PMA4 85=0.4647
C B0_d mass and lifetime, PDG96
```

```
PMA1 107=5.2792
PMA4 107=0.468
C B*0_d mass = M(B0_d)+45.7 MeV
PMA1 127=5.325
C B+ mass and lifetime, PDG96
PMA1 108=5.2789
PMA4 108=0.486
C B*+ mass = M(B+)+45.7 MeV
PMA1 128=5.325
C B0_s mass and lifetime, PDG96
PMA1 109=5.3693
PMA4 109=0.483
C B*0_s mass = M(B0_s)+45.7 MeV
PMA1 129=5.415
C B+_c mass and lifetime, estimated values (Eichen-Quigg, Masetti-Lusignoli)
PMA1 110=6.264
PMA4 110=0.150
C B*+_c mass, estimated value
PMA1 130=6.337
C Lambda_b mass, PDG96(UA1)+ALEPH96+DELPHI96
C Lambda_b lifetime, PDG96
PMA1 322=5.645
PMA4 322=0.342
C Assume lifetimes of Xib-,Xib0 and Omegab same as Lambdab
PMA4 324=0.342 325=0.342 356=0.342
C
C------------------------------------------------------------
C *** ALEPH tuning for B** production and decays from 1995 ***
C
C B*, B** production rates
PARJ 13=0.75 14=0.30 15=0.033 16=0.100 17=0.167
C
C Masses and widths of L=1 B mesons (id. by compressed codes KC)
C B0_1 mass and width, and max. deviation from nominal mass
PMA1 147=5.742
PMA2 147=0.021
PMA3 147=0.100
C B+_1 mass and width
PMA1 148=5.742
PMA2 148=0.021
PMA3 148=0.100
C B0_1s mass and width
PMA1 149=5.874
PMA2 149=0.001
PMA3 149=0.010
C B*0_0 mass and width
PMA1 167=5.63
PMA2 167=0.10
PMA3 167=0.20
C B*+_0 mass and width
PMA1 168=5.63
PMA2 168=0.10
PMA3 168=0.20
C B*0_0s mass and width
PMA1 169=5.762
PMA2 169=0.001
PMA3 169=0.100
C B*0_1 mass and width
PMA1 187=5.642
PMA2 187=0.100
PMA3 187=0.150
C B*+_1 mass and width
PMA1 188=5.642
PMA2 188=0.100
PMA3 188=0.150
```

```
C B*0_1s mass and width
PMA1 189=5.774
PMA2 189=0.001
PMA3 189=0.100
C B*0_2 mass and width
PMA1 207=5.754
PMA2 207=0.025
PMA3 207=0.100
C B*+_2 mass and width
PMA1 208=5.754
PMA2 208=0.025
PMA3 208=0.100
C B*0_2s mass and width
PMA1 209=5.886
PMA2 209=0.004
PMA3 209=0.050
C
C Branching ratios
C B0_1 decay probabilities to B*+pi- and B*0pi0
*DMOD 10513 753 1 0 0.667
*DMOD 10513 754 1 0 0.333
C B+_1 decay probabilities to B*0pi+ and B*+pi0
*DMOD 10523 755 1 0 0.667
*DMOD 10523 756 1 0 0.333
C B0_1s decay probabilities to B*+K- and B*0K0
*DMOD 10533 757 1 0 0.667
*DMOD 10533 758 1 0 0.333
C B*0_0 decay probabilities to B+pi- and B0pi0
*DMOD 10511 785 1 0 0.667
*DMOD 10511 786 1 0 0.333
C B*+_0 decay probabilities to B0pi+ and B+pi0
*DMOD 10521 787 1 0 0.667
*DMOD 10521 788 1 0 0.333
C Change B*0_0s decay to B*s gamma and disable other decays
*DMOD 10531 789 1 0 1.000 533 22 0 0 0
*DMOD 10531 790 0 0 0.000
C B*0_1 decay probabilities to B*+pi- and B*0pi0
*DMOD 20513 823 1 0 0.667
*DMOD 20513 824 1 0 0.333
C B*+_1 decay probabilities to B*0pi+ and B*+pi0
*DMOD 20523 825 1 0 0.667
*DMOD 20523 826 1 0 0.333
C Change B*0_1s decay to Bs gamma and B*s gamma
*DMOD 20533 827 1 0 0.500 531 22 0 0 0
*DMOD 20533 828 1 0 0.500 533 22 0 0 0
C B*0_2 decay probabilities to B+pi-, B0pi0, B*+pi-, B*0pi0,
C disable 3-body decays
*DMOD 515 904 1 0 0.3335
*DMOD 515 905 1 0 0.1665
*DMOD 515 906 1 0 0.3335
*DMOD 515 907 1 0 0.1665
*DMOD 515 908 0 0 0.
*DMOD 515 909 0 0 0.
*DMOD 515 910 0 0 0.
*DMOD 515 911 0 0 0.
C B*+_2 decay probabilities to B0pi+, B+pi0, B*0pi+, B*+pi0,
C disable 3-body decays
*DMOD 525 912 1 0 0.3335
*DMOD 525 913 1 0 0.1665
*DMOD 525 914 1 0 0.3335
*DMOD 525 915 1 0 0.1665
*DMOD 525 916 0 0 0.
*DMOD 525 917 0 0 0.
*DMOD 525 918 0 0 0.
*DMOD 525 919 0 0 0.
```

```
C B*0_2s decay probabilities to B+K-, B0K0, B*+K-, B*0K0
*DMOD 535 920 1 0 0.3335
*DMOD 535 921 1 0 0.1665
*DMOD 535 922 1 0 0.3335
*DMOD 535 923 1 0 0.1665
C------------------------------------------------------------
C End of datacards
END
```